

# NATIVE AND LIGHT INDUCED DEFECT STATES IN WIDE BAND GAP HYDROGENATED AMORPHOUS SILICON-CARBON( $a\text{-Si}_{1-x}\text{C}_x\text{:H}$ ) ALLOY THIN FILMS

MEHMET GÜNEŞ

*İzmir Institute of Technology, Faculty of Science, Department of Physics,  
Gaziosmanpaşa Bulv. No:16, Çankaya, İzmir, 35210-TURKEY.*

## 1. Abstract

In this study, wide band gap  $a\text{-Si}_{1-x}\text{C}_x\text{:H}$  alloy thin films prepared with and without hydrogen dilution of ( $\text{SiH}_4 + \text{CH}_4$ ) were characterized using optical absorption, dark conductivity, steady-state photoconductivity, sub-bandgap absorption obtained with both photothermal deflection spectroscopy (PDS) and dual beam photoconductivity (DBP), and electron spin resonance (ESR) techniques. Experimental results of steady-state photoconductivity and sub-bandgap absorption for different generation rates were analyzed using a detailed numerical model based on Simmons-Taylor statistics. The densities, energy location and nature of the native and light induced defect states in diluted and undiluted  $a\text{-Si}_{1-x}\text{C}_x\text{:H}$  alloy thin films were derived from the best fits to the experimental data. The extracted parameters for defect states were compared with those of  $a\text{-Si:H}$  films both in the annealed and light degraded states.

## 2. Introduction

High quality, wide band gap hydrogenated amorphous silicon-carbon ( $a\text{-Si}_{1-x}\text{C}_x\text{:H}$ ) alloy thin films are desired for use as an intrinsic layer in the top cell of multijunction solar cells [1] and as p-type layers of these and other electronic devices. It is well known that these materials can be prepared using glow discharge decomposition of silane and hydrocarbons such as methane ( $\text{CH}_4$ ) [2,-5] or using sputtering techniques [5]. However, these wide band gap  $a\text{-Si}_{1-x}\text{C}_x\text{:H}$  alloy materials were not so photosensitive. As the concentration of carbon in the film increases, dark and photoconductivity decrease, the density of localized defect states increases so do the optical gap and inverse slope of valence band tails,  $E_{ov}$  [2-6]. Alternatively, it was reported that the wide band gap  $a\text{-Si}_{1-x}\text{C}_x\text{:H}$  alloys prepared using  $\text{H}_2$ -dilution of ( $\text{SiH}_4 + \text{CH}_4$ ) gas mixture significantly improved the optoelectronic properties [7]. Later, this was supported by the studies of Baker et al. [8] and Li et al [9], who also reported that hydrogen dilution improved both dark and photoconductivity by several orders of magnitude. Recently, Lu et al. carried out more detailed studies on the process-property relations of  $a\text{-Si}_{1-x}\text{C}_x\text{:H}$  alloys deposited in PECVD system as a function of  $\text{H}_2$ -dilution ratio [10,11]. They reported that an increase in  $\text{H}_2$ -dilution resulted in an increase in surface smoothing, an increase in

the electron  $\mu\tau$  products, and a decrease in the sub-bandgap absorption, a decrease in the inverse slope of valence band tails,  $E_{ov}$ , and a decrease in the void fraction. They obtained optimum optoelectronic and microstructural properties of a-Si<sub>1-x</sub>C<sub>x</sub>:H alloys for dilution ratios of 20 to 24. Moreover, p-i-n homojunction solar cells prepared using diluted undoped a-Si<sub>1-x</sub>C<sub>x</sub>:H alloy layers showed high open-circuit voltages ( $V_{oc}$ ) and high fill factors [9].

Even though there were improvements in the optoelectronic properties, the defect states in a-Si<sub>1-x</sub>C<sub>x</sub>:H alloy thin films have not been studied and well characterized as extensively as those in a-Si:H thin films. Generally, electron spin resonance (ESR) [5], constant photo current method (CPM) [12], and photothermal deflection spectroscopy (PDS) [6,8,9] have been used. The density of defect states were derived either from the integration of CPM and PDS spectrum using the same integration constants, which were derived for a-Si:H thin films not for a-Si<sub>1-x</sub>C<sub>x</sub>:H alloys, or directly from ESR spins [3,5]. Due to higher density of surface/interface defect states, both ESR and PDS cannot be used for a reliable characterization of the bulk native defects in the annealed state. Alternatively, an approach of deconvolution of PDS and CPM spectrum was also used to obtain the distribution of defect states in the band gap [13]. However, this method ignores conduction band tails and does not take into account the presence of different defect states with different nature.

In addition, wide band gap a-Si<sub>1-x</sub>C<sub>x</sub>:H alloys also have intrinsic property of light induced degradation known as the Staebler-Wronski effect [14]. This has not been studied in detail yet and it is essential to determine long term stability of a-Si<sub>1-x</sub>C<sub>x</sub>:H based solar cells. Therefore, detailed characterizations of native and light induced defect states are necessary to understand the origins of these defects and mechanism for the Staebler-Wronski effect in wide band gap a-Si<sub>1-x</sub>C<sub>x</sub>:H alloys.

In this paper, wide band gap hydrogenated amorphous silicon-carbon alloy thin films prepared with and without H<sub>2</sub>-dilution of (SiH<sub>4</sub> + CH<sub>4</sub>) were studied using optical spectroscopy, dark and photo conductivity, and sub-bandgap absorption obtained with dual beam photoconductivity (DBP) technique [15] both in the annealed and light degraded states. The experimental results of photoconductivity and sub-bandgap absorption spectra were analyzed using a detailed numerical model described elsewhere [16].

### 3. Experimental Details

Steady-state photoconductivity and sub-bandgap absorption measurements were carried out on around 1  $\mu\text{m}$  thick undoped a-Si<sub>1-x</sub>C<sub>x</sub>:H alloy thin films deposited on 7059 glass substrate. Deposition conditions for these films were discussed elsewhere [9-11]. Optical absorption in the visible region of the spectrum was obtained from the transmission (T) and reflection (R) measurements and used to normalize sub-bandgap photoconductivities. The optical gaps were derived from the Tauc relation [17]. The ESR measurements were carried out on films codeposited onto quartz substrates. The annealed state was obtained by heating the samples at 200 °C for 12h in N<sub>2</sub> ambient and stabilized light soaked state was obtained by illuminating through both sides of the samples for more than 300h with 1W/cm<sup>2</sup> white light from an ELH light source filtered with both an IR reflector and IR absorber. Light soaking

temperature was maintained around 40°C for high intensity light soaking by air cooling through both sides of samples. Steady-state photoconductivities were measured in the ohmic regime with generation rate  $G=10^{15}$  to  $10^{20}$   $\text{cm}^{-3}\text{s}^{-1}$  using volume absorbed light of  $\lambda=620$  nm. The sub-bandgap photoconductivities, measured using dual beam photoconductivity (DBP) [15,16] technique with volume generation rates from  $G=10^{16}$  to  $10^{18}$   $\text{cm}^{-3}\text{s}^{-1}$ , were also carried out in the ohmic regimes of photocurrents.

## 4. Results

### 4.1. ANNEALED STATE

Undoped a-Si<sub>1-x</sub>C<sub>x</sub>:H alloy thin films were deposited at 300°C from decomposition of CH<sub>4</sub> and SiH<sub>4</sub> and dilution ratio (H<sub>2</sub>/(CH<sub>4</sub> + SiH<sub>4</sub>)) was 0:1 and 20:1. The optical gap obtained from the Tauc relation is 1.90 eV for both diluted and undiluted a-Si<sub>1-x</sub>C<sub>x</sub>:H films, which are higher than that of intrinsic a-Si:H film. The activation energies are 0.90 eV for undiluted and 0.98 eV for diluted a-Si<sub>1-x</sub>C<sub>x</sub>:H film which indicate that both films have the Fermi level close to middle of the gap.

The experimental results of the electron  $\mu\tau$  products in the annealed state are presented as a function of generation rate with open symbols in Figure 1. The generation rate dependence of  $\sigma_{\text{ph}} (\propto G^\gamma)$  is similar to that observed in a-Si:H films.  $\gamma$  is 0.86 for diluted, 0.80 for undiluted a-Si<sub>1-x</sub>C<sub>x</sub>:H, and 0.90 for intrinsic a-Si:H. It is clearly observed that undiluted a-Si<sub>1-x</sub>C<sub>x</sub>:H film has the electron  $\mu\tau$  products almost two orders of magnitude lower than those of intrinsic a-Si:H film. However, H<sub>2</sub>-dilution technique developed by Matsuda[7] improves the optoelectronic properties significantly [7-11]. The values of the electron  $\mu\tau$  products of diluted a-Si<sub>1-x</sub>C<sub>x</sub>:H film increased and became very close to those of intrinsic a-Si:H, which are shown in Figure 1. This has been attributed to a decrease in the densities of defect states in the bandgap.

The defect states in a-Si<sub>1-x</sub>C<sub>x</sub>:H films prepared with and without H<sub>2</sub>-dilution were investigated using the sub-bandgap absorption measured by DBP technique at different generation rates. These results are presented in Figure 2 for both films. The  $\alpha(h\nu)$  measured using PDS on the same a-Si<sub>1-x</sub>C<sub>x</sub>:H films in the annealed state are also shown in this Figure. It is important to note that PDS results are much higher than those measured by DBP and it also overestimates the  $E_{\text{ov}}$  because PDS detects all possible optical transitions to and from the defect states and those due to surface/interface defect states. The  $E_{\text{ov}}$  is 68 meV for diluted and 70 meV for undiluted film as determined from PDS measurements and corresponding DBP results are 55 and 60 meV for diluted and undiluted films, respectively.

As expected, the sub-bandgap absorption due to bulk defect states measured by low generation rate DBP is higher for undiluted a-Si<sub>1-x</sub>C<sub>x</sub>:H, i.e.  $\alpha(1.3\text{eV})$  is 1.1  $\text{cm}^{-1}$  and decreased to 0.35  $\text{cm}^{-1}$  for diluted a-Si<sub>1-x</sub>C<sub>x</sub>:H, which is very close to that of intrinsic a-Si:H film. The generation rate dependence of sub-bandgap absorption,  $\Delta\alpha(1.1\text{eV})$  [ $\Delta\alpha(1.1\text{eV})=\alpha(1.1\text{eV})$  measured by high G -  $\alpha(1.1\text{eV})$  measured by low G], is 0.11  $\text{cm}^{-1}$  for undiluted film and 0.14  $\text{cm}^{-1}$  for diluted a-Si<sub>1-x</sub>C<sub>x</sub>:H film. These are almost similar to those

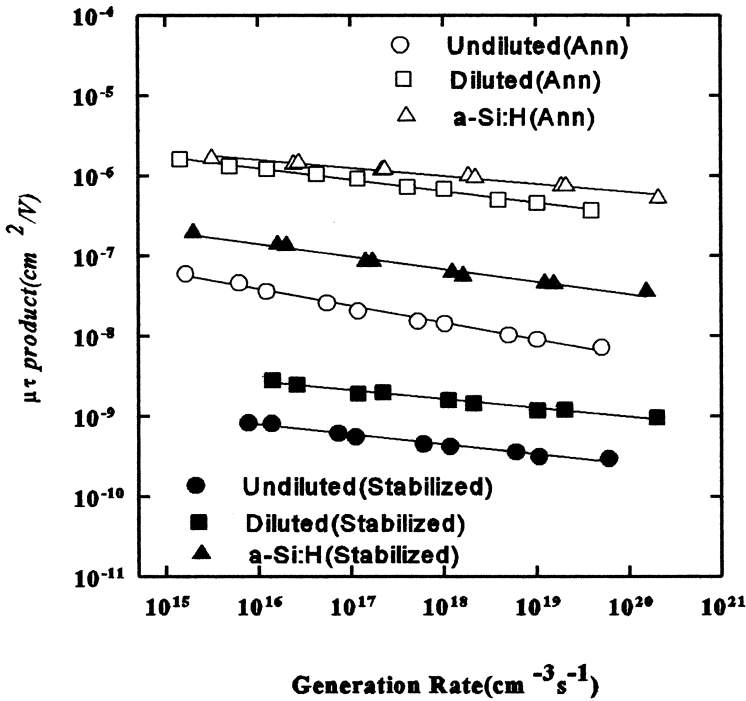


Figure 1. The electron  $\mu\tau$  products versus generation rates for diluted and undiluted  $a\text{-Si}_{1-x}\text{C}_x\text{:H}$  films and for an intrinsic  $a\text{-Si:H}$  film in the annealed and stabilized light soaked states.

measured in intrinsic  $a\text{-Si:H}$  films[18, 19] and much lower than those of non-intrinsic  $a\text{-Si:H}$  films, which have large densities of charged defect states[20]. Although undiluted film has a factor of 3 higher value of  $\alpha(1.3\text{eV})$  than diluted  $a\text{-Si}_{1-x}\text{C}_x\text{:H}$ , there is a factor of 35 differences between the electron  $\mu\tau$  products of diluted and undiluted films. This indicates that there could be possible differences in either the nature of defect states or free carrier mobilities or both in diluted and undiluted  $a\text{-Si}_{1-x}\text{C}_x\text{:H}$  films.

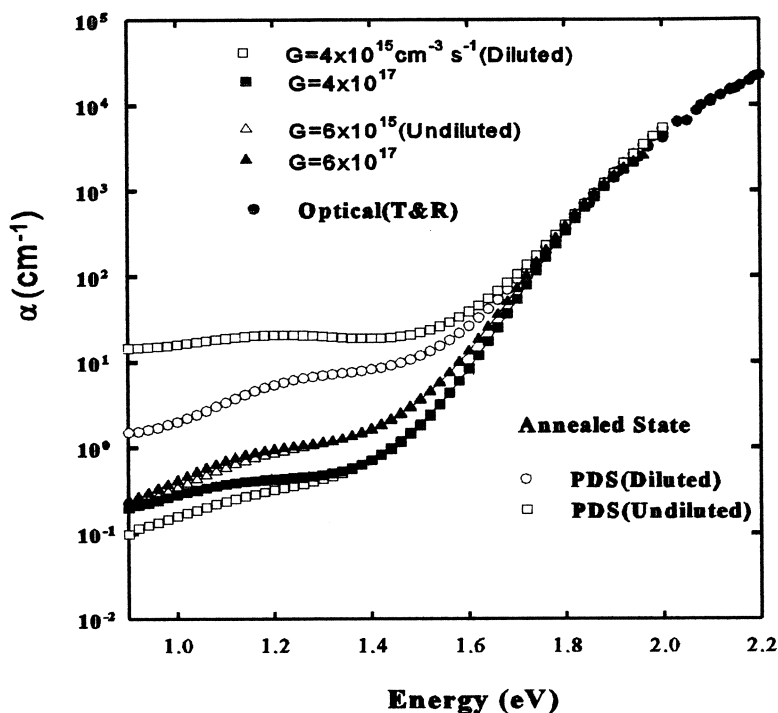


Figure 2. The  $\alpha(h\nu)$  versus energy measured by DBP at two generation rates and by PDS for diluted and undiluted  $a\text{-Si}_{1-x}\text{C}_x\text{:H}$  alloy thin films in the annealed state.

## 4.2 LIGHT SOAKED STATE

Although hydrogenated amorphous silicon-carbon alloys exhibit similar light induced instability, the Staebler-Wronski effect [14], they are less stable than  $a\text{-Si:H}$  films. In this study,  $a\text{-Si}_{1-x}\text{C}_x\text{:H}$  alloy films were light soaked up to the stabilized soaked state using high intensity,  $1\text{ W/cm}^2$ , ELH white light source. Experimental results of the electron  $\mu\tau$  products in the stabilized soaked state are shown as filled symbols in Figure 1 and those of sub-bandgap absorption are shown in Figures 3. The results are also summarized in Table 1 for diluted and undiluted  $a\text{-Si}_{1-x}\text{C}_x\text{:H}$  alloys as well as those of an intrinsic  $a\text{-Si:H}$  film.

Even though the electron  $\mu\tau$  products measured at  $G=10^{16}\text{ cm}^{-3}\text{s}^{-1}$  were similar for diluted  $a\text{-Si}_{1-x}\text{C}_x\text{:H}$  and intrinsic  $a\text{-Si:H}$  films in the annealed state, it decreased more drastically in diluted  $a\text{-Si}_{1-x}\text{C}_x\text{:H}$ . As seen in Figure 3, both diluted and undiluted  $a\text{-Si}_{1-x}\text{C}_x\text{:H}$  films exhibit much lower electron  $\mu\tau$  products than intrinsic  $a\text{-Si:H}$  in the stabilized soaked state. However,  $\gamma$  changes to around 0.85, which is similar to those observed in  $a\text{-Si:H}$  films

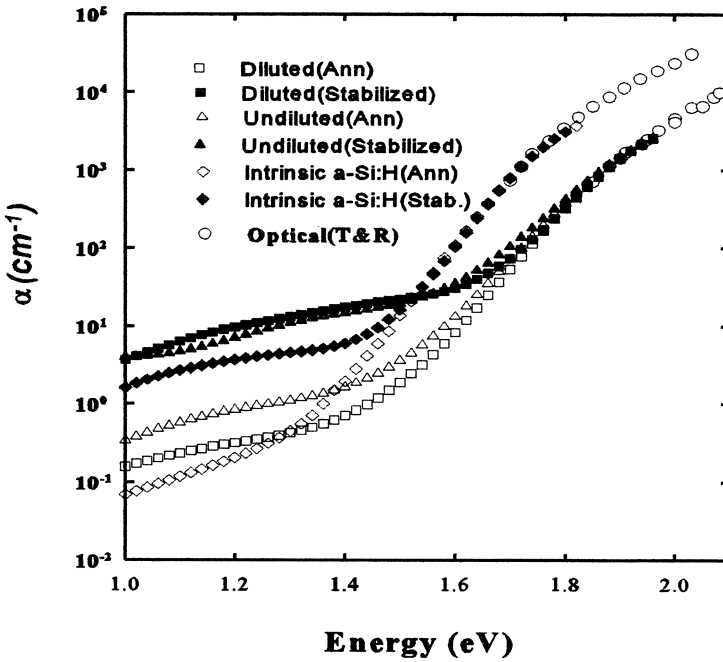


Figure 3. The sub-bandgap absorption spectra measured using DBP at low G for diluted and undiluted  $a\text{-Si}_{1-x}\text{C}_x\text{:H}$  films as well as those for intrinsic  $a\text{-Si:H}$  film both in the annealed and stabilized soaked states.

in the light soaked state [20]. This indicates that the distributions of the light induced defect states are similar in  $a\text{-Si}_{1-x}\text{C}_x\text{:H}$  alloys and  $a\text{-Si:H}$  films but the densities of light induced defect states must be significantly higher in  $a\text{-Si}_{1-x}\text{C}_x\text{:H}$  films to compensate the large degradation in the electron  $\mu\tau$  products.

Changes in the densities of light induced defect states were characterized using the sub-bandgap absorption in the stabilized soaked state. The results of  $\alpha(h\nu)$  for diluted and undiluted  $a\text{-Si}_{1-x}\text{C}_x\text{:H}$  and that for intrinsic  $a\text{-Si:H}$  are shown in Figure 3 both in the annealed and stabilized light soaked states. Although there is no detectable change in the slope of the valence band tail absorption for diluted  $a\text{-Si}_{1-x}\text{C}_x\text{:H}$  and  $a\text{-Si:H}$  film, there is slight increase in  $E_{0V}$  for undiluted film. It increased from 60 meV to 70 meV. The values of  $\alpha(1.3\text{eV})$  for diluted and undiluted  $a\text{-Si}_{1-x}\text{C}_x\text{:H}$  films are comparable in the stabilized state but they are a factor of 4 to 5 higher than that of intrinsic  $a\text{-Si:H}$ . In addition, the  $\Delta\alpha(1.1\text{eV})$  for diluted  $a\text{-Si}_{1-x}\text{C}_x\text{:H}$  increased from  $0.14\text{ cm}^{-1}$  to  $1.7\text{ cm}^{-1}$ , which is also higher than those measured in  $a\text{-Si:H}$  films. This indicates that the densities of light induced defect states in  $a\text{-Si}_{1-x}\text{C}_x\text{:H}$

Table 1. The experimental results of diluted and undiluted a-Si<sub>1-x</sub>C<sub>x</sub>:H films and those of intrinsic a-Si:H film both in the annealed and stabilized light soaked states. Where  $N_{\text{DOS}} = \alpha(1.3\text{eV}) \times 3 \times 10^{16}$  for a-Si<sub>x</sub>C<sub>1-x</sub>:H and  $N_{\text{DOS}} = \alpha(1.2\text{eV}) \times 3 \times 10^{16}$  for a-Si:H.

Films	Undiluted a-Si <sub>1-x</sub> C <sub>x</sub> :H	Diluted a-Si <sub>1-x</sub> C <sub>x</sub> :H	Intrinsic a-Si:H
$E_{\text{opt}}(\text{eV})$	1.90	1.90	1.72
$E_{\text{A}}(\text{eV})$	0.90	0.98	0.90
$\gamma(\text{Ann})$	0.80	0.86	0.90
$\gamma(\text{Soak})$	0.85	0.85	0.85
$\mu\tau(G=10^{16} \text{ cm}^{-3}\text{s}^{-1})$ (cm <sup>2</sup> /V)(Ann)	$3.6 \times 10^{-8}$	$1.2 \times 10^{-6}$	$1.5 \times 10^{-6}$
$\mu\tau(G=10^{16} \text{ cm}^{-3}\text{s}^{-1})$ (cm <sup>2</sup> /V)(Soak)	$8 \times 10^{-10}$	$2.8 \times 10^{-9}$	$1.5 \times 10^{-7}$
$\alpha(1.3\text{eV}) (\text{cm}^{-1})$ (Ann)	1.1	0.35	$\alpha(1.2)=0.16$
$\alpha(1.3\text{eV}) (\text{cm}^{-1})$ (Soak)	11.2	13.3	$\alpha(1.2)=3.7$
$N_{\text{DOS}}(\text{cm}^{-3})$ (Annealed)	$3.3 \times 10^{16}$	$1.05 \times 10^{16}$	$4.8 \times 10^{15}$
$N_{\text{DOS}}(\text{cm}^{-3})$ (Soaked)	$3.4 \times 10^{17}$	$4.0 \times 10^{17}$	$1.1 \times 10^{17}$
$N(\text{ESR}) (\text{cm}^{-3})$ (Soaked)	$4.1 \times 10^{17}$	$4.5 \times 10^{17}$	$1.0 \times 10^{17}$
$E_{\text{ov}}(\text{meV})(\text{Ann.})$	60	55	49
$E_{\text{ov}}(\text{meV})(\text{Soaked})$	70	56	49
$\Delta\alpha(1.3\text{eV})(\text{cm}^{-1})$ (Annealed)	0.11	0.14	0.06
$\Delta\alpha(1.3\text{eV}) (\text{cm}^{-1})$ (Soaked)	----	1.7	0.8

films, below as well as above the Fermi level, are higher than those in a-Si:H films. This was supported by the dark ESR spin density measurements carried out in the stabilized soaked state on both a-Si<sub>1-x</sub>C<sub>x</sub>:H and intrinsic a-Si:H films. It was found that the dark ESR spin signal comes from the same defect states with the same g number, 2.0055 [21]. The density of bulk defect states were significantly higher than that of surface/interface defect states present in the annealed state [18]. The absolute density of ESR spins (after subtracting the density of surface/interface defect states) is  $1.0 \times 10^{17} \text{ cm}^{-3}$  for a-Si:H,  $4.5 \times 10^{17} \text{ cm}^{-3}$  for diluted, and  $4.1 \times 10^{17}$  for undiluted a-Si<sub>1-x</sub>C<sub>x</sub>:H. The densities of defect states below the Fermi level can also be obtained from sub-bandgap absorption using the values of  $\alpha(1.3 \text{ eV})$  [18]. It is  $3.5 \times 10^{17} \text{ cm}^{-3}$  for undiluted,  $4.0 \times 10^{17} \text{ cm}^{-3}$  for diluted a-Si<sub>1-x</sub>C<sub>x</sub>:H alloy and  $1.1 \times 10^{17} \text{ cm}^{-3}$  for a-Si:H film. These values agree very well with those measured directly using ESR. Even though the densities of the D<sup>0</sup> states are factor of 4-5 higher in a-Si<sub>1-x</sub>C<sub>x</sub>:H alloys, the electron  $\mu\tau$  products in the stabilized state were lower by a factor of 54 for diluted and 187 for undiluted a-Si<sub>1-x</sub>C<sub>x</sub>:H. These large differences in the degradation of the electron  $\mu\tau$  products can be attributed to the increases in the densities of other type defect states such as charged Si dangling bonds as in a-Si:H films or possibly any carbon related light induced defect states. This can only be possible through a detailed analysis of the experimental results both in the annealed and light soaked states.

## 5. Native Defect States in a-Si<sub>1-x</sub>C<sub>x</sub>:H Alloys

The defect states in hydrogenated amorphous silicon-carbon alloys have not been studied as extensively as those in a-Si:H materials. In 1982, Morimoto et al. [5] reported that ESR spins were due to silicon and carbon dangling bonds depending on the carbon content in the film where for  $x$  ( $x = C_{\text{carbon}} / (C_{\text{carbon}} + C_{\text{Si}})$ ) less than 0.2,  $g$  is 2.0055, the same as the neutral Si dangling bonds. The same group also found that the density of charged defect states in a-Si:H obtained from LESR decreased with carbon alloying but increased with O and N alloying [12].

In 1992, Robertson reported a theoretical study of defect states in a-Si<sub>1-x</sub>C<sub>x</sub>:H alloys using the tight binding approximation [22]. It was found that for  $x < 0.5$ , Si dangling bond defects and  $x > 0.6$  carbon dangling bond defects dominate in the alloy, but no charged defect states resulted from these calculations. The nature of tail states were like those of a-Si:H, i.e. the valence band tails are wider than the conduction band tail states.

Since a-Si<sub>1-x</sub>C<sub>x</sub>:H alloy films studied here were Si rich and they were treated like a-Si:H films. The concentration of carbon in these alloys determined from electron probe microanalysis was less than 0.1 at.% [11]. Preliminary results of the analysis on diluted and undiluted a-Si<sub>1-x</sub>C<sub>x</sub>:H films were presented assuming the same distribution of the gap states and charged defect states as used in a-Si:H films [18]. The distribution used in the modeling consists of parabolic extended states, exponential valence and conduction band tail states, two Gaussian distributions of neutral and negatively charged states located below the Fermi level and a Gaussian distribution of positively charged states located above the Fermi level [18]. The results of photoconductivities and sub-bandgap absorption were analyzed using sub-



bandgap absorption model (SAM) [16,19]. This model is based on Simmons-Taylor statistics [23], which was developed for a continuous distribution of gap states in the bandgap of insulators. In the modeling, the parameters for the extended states, tail states, and carrier capture cross-sections of the defect states were assumed to be the same as those in a-Si:H films. Experimental values of the optical gap, the Fermi level position, and  $E_{ov}$ (meV) were important inputs in the modeling. The mobility gaps were assumed to be 0.18 eV larger than optical gap. Because the electron  $\mu\tau$  products in diluted a-Si<sub>1-x</sub>C<sub>x</sub>:H and intrinsic a-Si:H film were virtually the same in the annealed state, the same free carrier mobilities were assumed as those used for a-Si:H. There was no any priory assumptions for the densities and energy location of the native defect states. These were derived from the self-consistent fits to the results of both  $\sigma_{ph}$  and sub-bandgap absorption in the annealed state.

The results(symbols) of the sub-bandgap absorption and  $\sigma_{ph}$  (in the inset) and the best fits (solid lines) are shown in Figure 4 for diluted and in Figure 5 for undiluted a-Si<sub>1-x</sub>C<sub>x</sub>:H films. It was found that the distribution of the charged defect states can be successfully used to fit the results of the diluted a-Si<sub>1-x</sub>C<sub>x</sub>:H. Even though it is possible to obtain equivalent fits

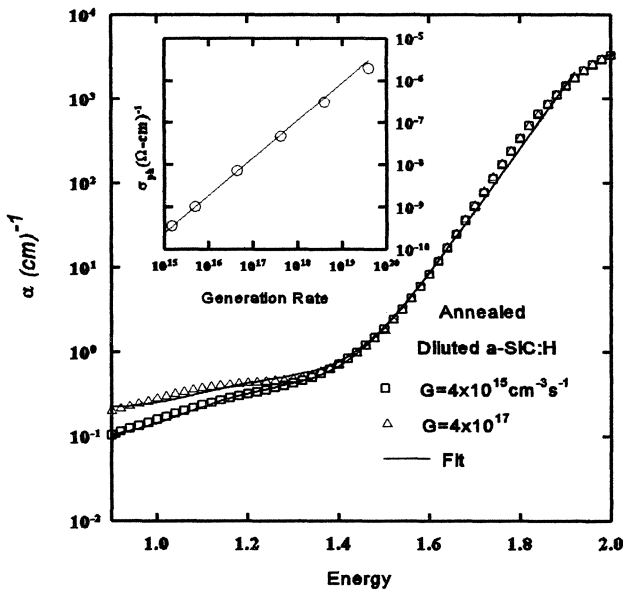


Figure 4. The sub-bandgap absorption spectra and  $\sigma_{ph}$  (inset) for diluted a-Si<sub>1-x</sub>C<sub>x</sub>:H film in the annealed state. The symbols are the experimental results and solid lines are the best fits to the data.

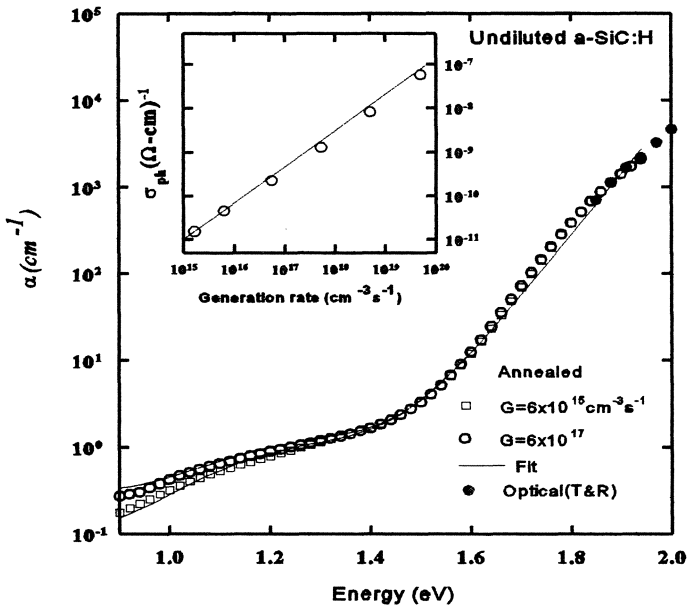


Figure 5. The sub-bandgap absorption spectra and  $\sigma_{ph}$  (inset) for undiluted a-Si<sub>1-x</sub>C<sub>x</sub>:H film in the annealed state. The symbols are the experimental results and solid lines are the best fits to the data.

to the sub-bandgap absorption spectra for two different generation rates, the values of steady-state photoconductivity in undiluted a-Si<sub>1-x</sub>C<sub>x</sub>:H alloy film cannot be matched using the same parameters of the gap states as used in diluted a-Si<sub>1-x</sub>C<sub>x</sub>:H. This requires to use a factor of 25 lower free electron and hole mobilities than those used for diluted alloy or to introduce different states, such as carbon related defect states with higher capture cross-sections or both to fit photoconductivities in the analysis. The densities and energy locations of the neutral and charged defect states in diluted film as well as those in intrinsic a-Si:H film are summarized in Table 2.

The densities of the neutral and charged defect states in diluted a-Si<sub>1-x</sub>C<sub>x</sub>:H film are higher than those of intrinsic a-Si:H film. This results in higher sub-bandgap absorption as well as higher  $\Delta\alpha(1.1\text{eV})$  for diluted a-Si<sub>1-x</sub>C<sub>x</sub>:H. The energy position of the defect states are found to be further away from the valence band edge in wide band gap a-Si<sub>1-x</sub>C<sub>x</sub>:H alloy. The ratio of the charged to neutral defect states,  $R = ([N_{D^+} + N_{D^-}] / N_{D_0})$ , is 1.0 for diluted a-Si<sub>1-x</sub>C<sub>x</sub>:H film, which is slightly lower than those obtained in intrinsic a-Si:H films studied earlier [19]. In conclusion, the distribution of charged defect states can be successfully applied to self-consistent analysis of steady-state photoconductivity and sub-bandgap absorption

spectra for diluted a-Si<sub>1-x</sub>C<sub>x</sub>:H alloys.

Table 2. The densities and energy locations of the native defect states derived from the analysis of  $\sigma_{ph}$  and  $\alpha(h\nu)$  spectra in diluted a-Si<sub>1-x</sub>C<sub>x</sub>:H and those for intrinsic a-Si:H film in the annealed states.  $N_{DOS}=3 \times 10^{16} \times \alpha(ref.)$ , where *ref.* is 1.2 eV for a-Si:H and 1.3 eV for a-Si<sub>1-x</sub>C<sub>x</sub>:H films. The extended state parameters and capture cross-sections for defect states are the same as those in ref [19].

Parameters	Diluted a-Si <sub>1-x</sub> C <sub>x</sub> :H Film	Intrinsic a-Si:H
$E_{opt}(eV)$	1.90	1.72
$E_F(eV)(\text{from CB})$	0.98	0.90
$E_{OV}(meV)$	55	49
$E_{OC}(meV)$	30	21
$E_{D0}(eV)$ from VB	0.90	0.78
Width(eV)	0.13	0.13
$N_{D0}(cm^{-3})$	$9 \times 10^{15}$	$4.5 \times 10^{15}$
$E_{D+}(eV)$ from VB	1.46	1.28
Width(eV)	0.1	0.08
$N_{D+}(cm^{-3})$	$4.5 \times 10^{15}$	$3 \times 10^{15}$
$E_{D-}(eV)$ from VB	0.60	0.50
Width(eV)	0.1	0.08
$N_{D-}(cm^{-3})$	$4.5 \times 10^{15}$	$3 \times 10^{15}$
$N_{DOS}(cm^{-3})$	$1.1 \times 10^{16}$	$4.8 \times 10^{15}$
$R=(N_{D+}+N_{D-})/N_{D0}$	1.0	1.4
$\mu_n(cm^2/Vsec)$	10	10
$\mu_p(cm^2/Vsec)$	1	1

## 6. Light Induced Defect States in a-Si<sub>1-x</sub>C<sub>x</sub>:H Alloys

It was shown that hydrogenated amorphous silicon-carbon alloys were less stable than a-Si:H films. Since they exhibited more degradation in  $\sigma_{ph}$  and large increase in  $\alpha(h\nu)$  in the stabilized soaked state. However, the degradation of  $\sigma_{ph}$  was not directly correlated with the increase of sub-bandgap absorption which is due to the increases in the densities of the dangling bond states below Fermi level. In order to understand the light induced degradation in these alloy films, the numerical analysis of  $\sigma_{ph}$  and  $\alpha(h\nu)$  were extended to the results of diluted and undiluted a-Si<sub>1-x</sub>C<sub>x</sub>:H films in the stabilized soaked state.

In the previous section, it was shown that the distributions of the charged defect states can be used to characterize the native defect states only in diluted a-Si<sub>1-x</sub>C<sub>x</sub>:H film but not for undiluted film. The same distribution of defect states is now used in the modeling of the light induced defect states where only changes in the densities of midgap states were assumed to occur with light soaking. The energy locations and capture cross-sections of defect states were maintained the same as those in the annealed state. The densities of the light induced defect states were derived from the best fits to the results of the  $\sigma_{ph}$  and  $\alpha(h\nu)$ . The experimental results (symbols) of  $\sigma_{ph}$  and  $\alpha(h\nu)$  and the best fits (solid lines) are shown in Figure 6 for diluted a-Si<sub>1-x</sub>C<sub>x</sub>:H film both in the annealed and stabilized soaked state. The densities of the neutral Si dangling bond states, the D<sup>0</sup>, are  $4.9 \times 10^{17} \text{ cm}^{-3}$ , which is close to the value of  $4.5 \times 10^{17} \text{ cm}^{-3}$ , the density of ESR spins measured on the same film in the stabilized state. It is factor of 4 to 5 higher than those measured in intrinsic a-Si:H. Although equally

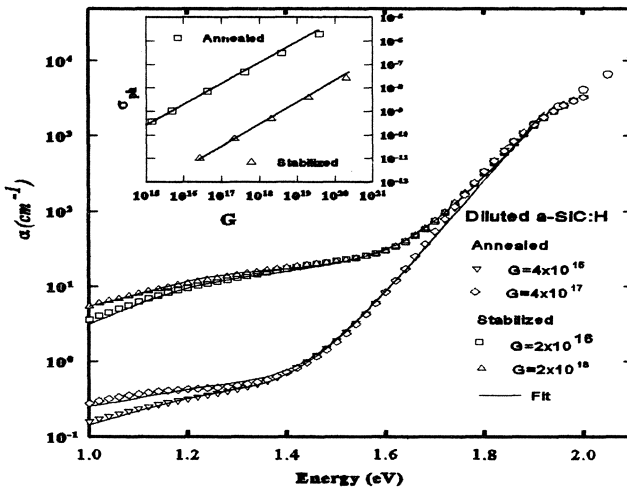


Figure 6. The sub-bandgap absorption spectra and  $\sigma_{ph}$  (inset) for diluted a-Si<sub>1-x</sub>C<sub>x</sub>:H film in the annealed and stabilized states. The symbols are the experimental results and solid lines are the best fits to the data.

good fits to the generation rate dependence of the sub-bandgap absorption were obtained using the densities of  $1.7 \times 10^{17} \text{ cm}^{-3}$  for both the  $D^+$  and the  $D^-$  states, these were not sufficient to fit the large decrease in the steady-state photoconductivities. In order to obtain the best fits to  $\sigma_{ph}$  for wide range of generation rates, a factor of 25 decrease in the free carrier mobilities were required in the stabilized light soaked state. In addition, even if the results of undiluted  $a\text{-Si}_{1-x}\text{C}_x\text{:H}$  film were fitted in the annealed state using the same distribution of charged defect states and with certain free carrier mobilities, it is also impossible to match the values of photoconductivities in the stabilized soaked state without decreasing free carrier mobilities by more than a factor of 40. This indicates that light induced defect states in diluted and undiluted  $a\text{-Si}_{1-x}\text{C}_x\text{:H}$  alloys are not the same as those in  $a\text{-Si:H}$  films. Even though the neutral Si dangling bond states, the  $D^0$ , created by light are the same both in  $a\text{-Si:H}$  and Si rich  $a\text{-Si}_{1-x}\text{C}_x\text{:H}$  alloys [21], different type of defect states with higher capture cross-sections could be created by light soaking in  $a\text{-Si}_{1-x}\text{C}_x\text{:H}$  alloys. Further studies are necessary to investigate the light induced defect states in  $a\text{-Si}_{1-x}\text{C}_x\text{:H}$  alloys and any possible changes in the transport properties with light soaking.

## 7. Conclusions

Preliminary results on device quality, one diluted and one undiluted,  $a\text{-Si}_{1-x}\text{C}_x\text{:H}$  film show that the distribution of charged defect states used in the analysis of  $a\text{-Si:H}$  films can be used to characterize the defect states in diluted  $a\text{-Si}_{1-x}\text{C}_x\text{:H}$  film in the annealed state. The densities of the neutral and charged defect states in diluted  $a\text{-Si}_{1-x}\text{C}_x\text{:H}$  are comparable with those in  $a\text{-Si:H}$  films. The ratio of the charged to neutral defect states is around 1.0 and slightly lower than those obtained in intrinsic  $a\text{-Si:H}$  films and much lower than those of undoped (non-intrinsic)  $a\text{-Si:H}$  films studied previously [20]. The lower values of  $R$  in  $a\text{-Si}_{1-x}\text{C}_x\text{:H}$  film are consistent with the experimental results of ESR and LESR carried out on  $a\text{-Si:H}$  and  $a\text{-Si}_{1-x}\text{C}_x\text{:H}$  materials reported by Shimizu et al. [12]. However, the results of undiluted  $a\text{-Si}_{1-x}\text{C}_x\text{:H}$  film in the annealed states cannot be analyzed using the same distributions and gap states parameters of diluted film. It was inferred that different type of defect states with higher capture cross-sections could be present in undiluted film and/or possible lower free carrier mobilities.

In the light soaked state, it was found that both diluted and undiluted  $a\text{-Si}_{1-x}\text{C}_x\text{:H}$  films are less stable than  $a\text{-Si:H}$  films. Self-consistent analysis of the results in the light soaked state was impossible even for diluted film using the same distribution of gap states and parameters used in the annealed state. Even though almost the same densities of the  $D^0$  states measured by ESR were used as input to fit low  $G$  sub-bandgap absorption spectrum, this was not sufficient to account for the light induced degradation in photoconductivities. Different type of light induced defect states which are not present in  $a\text{-Si:H}$  film and/or lower free carrier mobilities or both are necessary to fit lower photoconductivities in both diluted and undiluted  $a\text{-Si}_{1-x}\text{C}_x\text{:H}$  alloys. Further research on the native and light induced defect states in

Si rich  $a\text{-Si}_{1-x}\text{C}_x$  :H alloys are necessary to understand the Staebler-Wronski effect in these materials.

## 8. Acknowledgements

Experimental part of this study was carried out at the Pennsylvania State University. It was supported by NREL under Subcontract No. XG-1-10063. The author would like to thank Drs. C.R.Wronski and R. W. Collins at the Pennsylvania State University for scientific collaborations and helpfull discussions, Drs. T.J. McMahon and R. Crandall of NREL for ESR and electron probe microanalysis experiments, and Dr. Yuan-Min Li of Solarex for PDS measurements. The author would also like to thank Turkish Government, Ministry of National Education for the partial Ph.D scholarship during his stay in the USA.

## 9. References

1. Kuwano, Y. (1986) *Plasma Deposited Thin Films*, edited by J.Mort and F. Jansen, CRC, Boca Raton, p. 161.
2. Paul, W. Paul, D. K., Von Roedern, B., Blake, J., and Oguz, S. (1981) *Phys. Rev. Lett.* **46**, 1016 .
3. Morimoto, A., Miura, T., Kumeda, M., and Shimizu, T. (1981) *Jpn. J. Appl. Phys.* **20**, L833.
4. Schmidt, M.P., Bullot, J., Gauthier, M., Cordier, P., Solomon, I., and Tran-Quoc, H. (1985) *Phil. Mag.* **B51**, 581.
5. Morimoto, A., Miura, T., Kumeda, M., and Shimizu, T. (1982) *J. Appl. Phys.* **53**, 7299.
6. Boulitrop, F., Bullot, J., Gauthier, M., Schmidt, M.P., Catherine, Y. (1985) *Solid State Comm.* **54**, 107.
7. Matsuda, A., and Tanaka, K. (1987) *J. Non-Cryst. Solids* **97&98**, 1367.
8. Baker, S. H., Spear, W. E., and Gibson, R. A. G. (1990) *Phil. Mag.* **B62**, 213.
9. Li, Yuan-Min., Catalano, A., Fieselmann, F. B. (1992) *Mat. Res. Soc. Symp. Proc.* **258**, 923.
10. Lu, Y., An, I., Gunes, M., Wakagi, M., Wronski, C.R., and Collins, R.W. (1993) *Appl. Phys. Lett.* **63**, 2228.
11. Lu, Y., Kim, S., Gunes, M., Lee, Y., Wronski, C.R., and Collins, R.W. (1994) *Mat. Res. Soc. Symp. Proc.* **336**, 595.
12. Shimizu, T., Kidoh, H., Morimoto, A., Kumeda, A. (1989) *Jap. J. Appl. Phys.* **28**, 586.
13. Demichelis, F., Crovini, G., Giorgis, F., Pirri, C.F., Tresso, E., Amato, G., Herremans, H., Grevendonk, W., Rava, P. (1993) *J. Non-Cryst. Solids* **164-166**, 1015.

- 14 Staebler, D.L., Wronski, C.R. (1977) *Appl. Phys. Lett.* **31**, 292.
- 15 Lee, S., Kumar, S., Wronski, C.R., and Maley, N. (1989) *J. Non-Cryst. Solids* **114**, 316.
- 16 Lee, S., Gunes, M., Wronski, C.R., Maley, N., and Bennett, M. (1991) *Appl. Phys. Lett.* **59**, 1578.
- 17 Tauc, J. (1972) in *Optical properties of Solids*, edited by F. Abeles, North Holland, New York, p.279.
- 18 Gunes, M., Wronski, C.R., and McMahon, T.J. (1994) *J. Appl. Phys.* **76**, 2260.
- 19 Gunes, M., Collins, R.W., and Wronski, C.R. (1994) *Mat. Res. Soc. Symp. Proc.* **336**, 413.
- 20 Gunes, M. (1995) *Ph. D.Thesis*, The Pennsylvania State University, University Park PA, USA.
- 21 McMahon, T.J. (1995) Private communication.
- 22 Robertson, J. (1992) *Phil. Mag.* **B66**, 615(1992).
- 23 Simmons, J.G., and Taylor, G.W. (1971) *Phys. Rev.* **B4**, 502.